



CHORUS

This is the accepted manuscript made available via CHORUS. The article has been published as:

Interlayer Pairing Symmetry of Composite Fermions in Quantum Hall Bilayers

Hiroki Isobe and Liang Fu

Phys. Rev. Lett. **118**, 166401 — Published 17 April 2017

DOI: [10.1103/PhysRevLett.118.166401](https://doi.org/10.1103/PhysRevLett.118.166401)

Interlayer pairing symmetry of composite fermions in quantum Hall bilayers

Hiroki Isobe and Liang Fu

Department of Physics, Massachusetts Institute of Technology, Cambridge, Massachusetts 02139, USA

We study the pairing symmetry of the interlayer paired state of composite fermions in quantum Hall bilayers. Based on the Halperin-Lee-Read (HLR) theory, the effect of the long-range Coulomb interaction and the internal Chern-Simons gauge fluctuation is analyzed with the random-phase approximation beyond the leading order contribution in small momentum expansion, and we observe that the interlayer paired states with a relative angular momentum $l = +1$ is energetically favored for filling $\nu = \frac{1}{2} + \frac{1}{2}$ and $\frac{1}{4} + \frac{1}{4}$. The degeneracy between states with $\pm l$ is lifted by the interlayer density-current interaction arising from the interplay of the long-range Coulomb interaction and the Chern-Simons term in the HLR theory.

Quantum Hall systems with even-denominator filling fractions are well described by composite fermions (CFs) [1]. A CF in two dimensions is composed of an electron with an even number of magnetic fluxes attached via the Chern-Simons gauge field. The attached fluxes cancel the external magnetic field on average, thus leading to a well-defined Fermi surface of CFs as theorized by Halperin, Lee, and Read [2].

In quantum Hall bilayer systems, quantized Hall conductances, indicative of incompressible states, are observed when each layer is at even-denominator filling fractions and two layers are separated by short distance. Such systems are realized in a single wide quantum well [3], double quantum wells [4], and more recently, bilayer graphene [5–8]. Tunneling spectroscopy [9, 10], Hall drag [11], and counterflow measurements [12, 13] demonstrate the formation of an exciton superfluid phase for small layer distances [14–16]. On the other hand, the bilayer system is described by two composite Fermi liquids with interlayer interactions at large distance. From a theoretical viewpoint, Bonesteel *et al.* [17, 18] showed that such a system is unstable to Cooper pairing between CFs on the two different layers. The pairing interaction arises from the long-range Coulomb interaction and fluctuations of the Chern-Simons gauge fields. Using the random-phase approximation (RPA) for the gauge field propagator, Refs. [17, 18] derived the most singular part of the pairing interaction. As recognized by the authors, at this level of approximation, pairing interactions in all angular momentum channels are degenerate.

In this paper, we study the energetically favored pairing symmetry of bilayer quantum Hall systems due to the effective interaction between CFs obtained by the RPA. We go beyond the previous analyses to include the effect of the time-reversal breaking external magnetic field on the effective interaction between CFs. This effect appears through an interlayer density-current interaction mediated by the Chern-Simons gauge field. The resulting pairing interaction between CFs lifts the degeneracy between pairings in angular momentum $+l$ and $-l$ channels. We show that the interlayer paired state with a relative angular momentum $l = +1$ is favored at filling

$\nu = \frac{1}{2} + \frac{1}{2}$ and $\frac{1}{4} + \frac{1}{4}$. Here we define the angular momentum of the Moore-Read Pfaffian state [19] as $l = +1$.

Model. We consider a bilayer system of CFs with layer spacing d in the presence of the long-range Coulomb interaction [Fig. 1(a)]. We assume that the filling fraction is the same for both layers. In the imaginary time formalism, the partition function is $Z = \int \prod_s D\psi_s^\dagger D\psi_s D\mathbf{a}^{(s)} D a_0^{(s)} e^{-S}$, with the action $S = \int_0^\beta d\tau \int d^2\mathbf{r} \mathcal{L}(\mathbf{r}, \tau)$. The Lagrangian density \mathcal{L} is given by [17, 18, 22]

$$\begin{aligned} \mathcal{L}(\mathbf{r}, \tau) &= \sum_s \left\{ \psi_s^\dagger(\mathbf{r}, \tau) \left[\partial_\tau + i a_0^{(s)}(\mathbf{r}, \tau) \right] \psi_s(\mathbf{r}, \tau) \right. \\ &\quad + \frac{1}{2m^*} \psi_s^\dagger(\mathbf{r}, \tau) \left[-i\nabla - \mathbf{a}^{(s)}(\mathbf{r}, \tau) + e\mathbf{A}(\mathbf{r}) \right]^2 \psi_s(\mathbf{r}, \tau) \\ &\quad \left. - \mu \psi_s^\dagger(\mathbf{r}, \tau) \psi_s(\mathbf{r}, \tau) \right\} \\ &\quad - \sum_{ss'} \frac{i}{2\pi} K_{ss'}^{-1} a_0^{(s)}(\mathbf{r}, \tau) \hat{z} \cdot [\nabla \times \mathbf{a}^{(s')}(\mathbf{r}, \tau)] \\ &\quad + \frac{1}{2} \sum_{ss'} \int d^2\mathbf{r}' \delta\rho_s(\mathbf{r}, \tau) V_{ss'}(\mathbf{r} - \mathbf{r}') \delta\rho_{s'}(\mathbf{r}', \tau), \quad (1) \end{aligned}$$

where ψ_s represents the CF field with $s = 1, 2$ (or \uparrow, \downarrow) being a layer index, m^* is the effective mass of the CFs, $\mathbf{a}^{(s)}$ and $a_0^{(s)}$ are the Chern-Simons gauge fields, and \mathbf{A} is the $U(1)$ gauge field for the uniform external magnetic field B along the z direction. Here we employ units where $\hbar = c = 1$, and the Coulomb gauge for the Chern-Simons gauge field; $\nabla \cdot \mathbf{a}^{(s)} = 0$. The electron charge is $-e$. The filling fraction of each layer is $2\pi n_e / (eB)$, where n_e is the electron density, and μ is the chemical potential. The energy dispersion is $\epsilon_{\mathbf{k}} = k^2 / (2m^*)$, and the Fermi wave vector k_F is given by $k_F = \sqrt{4\pi n_e} = \sqrt{2\nu} / l_0$, where the magnetic length is $l_0 = (eB)^{-1/2}$. The Coulomb interaction $V_{ss'}(\mathbf{r}) = e^2 / (\epsilon r)$ ($s = s'$) or $e^2 / (\epsilon \sqrt{r^2 + d^2})$ ($s \neq s'$) [20] acts on the density fluctuation $\delta\rho_s(\mathbf{r}, \tau) = \psi_s^\dagger(\mathbf{r}, \tau) \psi_s(\mathbf{r}, \tau) - n_e$. The elements of the K matrix are taken as $K_{11} = K_{22} = \tilde{\phi}$ and $K_{12} = K_{21} = 0$, with the integer $\tilde{\phi}$ corresponding to the number of fluxes attached to an electron. This is confirmed by integrating out $a_0^{(s)}$,

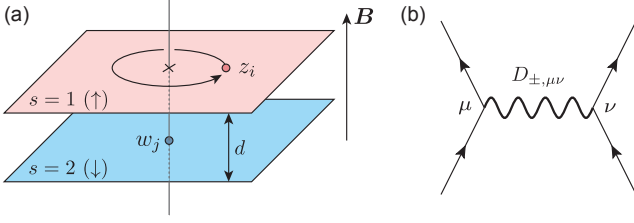


FIG. 1: (a) Geometry of the bilayer system. The magnetic field \mathbf{B} is applied upward through the two layers with the distance d . An interlayer paired state with a relative angular momentum l gives a winding phase $2\pi l$ when one moves a CF counterclockwise around another in the other layer. (b) Effective interaction for CFs. $\mu = 0$ (1) at a vertex means a coupling between the density (current) fluctuation of CFs and the Chern-Simons gauge field.

to obtain the constraint $\psi_s^\dagger \psi_s = \hat{z} \cdot \nabla \times \mathbf{a}^{(s)} / (2\pi\tilde{\phi})$. Note that the sign of $\tilde{\phi}$ represents the direction of the magnetic field, and it changes by time-reversal operation; we take $\tilde{\phi} > 0$ in the following analysis to make the direction of the magnetic field point upward. The filling fraction of each layer is $\tilde{\phi}^{-1}$, so that the CFs feel effectively no magnetic field on average. The density fluctuation is given by

$$\delta\rho_s(\mathbf{r}, \tau) = \frac{1}{2\pi\tilde{\phi}} \hat{z} \cdot \nabla \times [\mathbf{a}^{(s)}(\mathbf{r}, \tau) - e\mathbf{A}(\mathbf{r})]. \quad (2)$$

Effective interaction. The effective action for the gauge field is obtained by a saddle-point approximation with expansion about the point where $a_0^{(s)} = 0$ and $\mathbf{a}^{(s)} - e\mathbf{A} = 0$. With the Coulomb gauge condition, the gauge fluctuation in the spatial part can be written by $a_1^{(s)}(\mathbf{q}, i\omega_m) = \hat{z} \cdot \hat{\mathbf{q}} \times [\mathbf{a}^{(s)}(\mathbf{q}, i\omega_m) - e\mathbf{A}(\mathbf{q})]$, where $\omega_m = 2m\pi T$ is a bosonic Matsubara frequency. Up to the second order in the gauge field, the effective action is

$$S_{\text{eff}} = \frac{1}{2} T \sum_{\omega_m} \int \frac{d^2q}{(2\pi)^2} \sum_{ss'} \sum_{\mu, \nu=0,1} a_\mu^{(s)}(\mathbf{q}, i\omega_m) \times D_{s\mu, s'\nu}^{-1}(q, i\omega_m) a_\nu^{(s')}(-\mathbf{q}, -i\omega_m). \quad (3)$$

It is useful for later analysis to decompose the gauge field into in-phase and out-of-phase fluctuations $a_\mu^{(\pm)} = (a_\mu^{(1)} \pm a_\mu^{(2)})/\sqrt{2}$, with the corresponding propagator $D_{\pm, \mu\nu}$. $D_{\pm, \mu\nu}^{-1}$ is obtained with the RPA [17, 18, 23, 24], whose singular terms for $\omega/\epsilon_F \ll (q/k_F)^2 \ll 1$ and

$q \ll d^{-1}$ are

$$D_{-,11}(q, i\omega_m) \approx -\frac{1}{\tilde{\chi}d q^2 + \frac{k_F}{2\pi} \frac{|\omega_m|}{q}}, \quad (4a)$$

$$D_{+,11}(q, i\omega_m) \approx -\frac{1}{\frac{e^2}{\pi\epsilon\tilde{\phi}^2} q + \frac{k_F}{2\pi} \frac{|\omega_m|}{q}}, \quad (4b)$$

$$D_{-,01}(q, i\omega_m) = D_{-,10}(q, i\omega_m) \approx \frac{1}{\tilde{\chi}d q^2 + \frac{k_F}{2\pi} \frac{|\omega_m|}{q}} \frac{q}{m^* \tilde{\phi}}, \quad (4c)$$

with $\tilde{\chi}d = \frac{1}{24\pi m^*} + \frac{e^2 d}{2\pi\epsilon\tilde{\phi}^2} + \frac{1}{2\pi m^* \tilde{\phi}^2}$.

From the effective action and the gauge propagator, the effective interaction between the CFs [Fig. 1(b)] is obtained by

$$\mathcal{V} = \frac{1}{2} \sum_{s_1 s_2 s_3 s_4} \psi_{s_1}^\dagger(\mathbf{k} + \mathbf{q}, i\epsilon_n + i\omega_m) \psi_{s_2}^\dagger(\mathbf{k}' - \mathbf{q}, i\epsilon'_n - i\omega_m) \times V_{s_1 s_2 s_3 s_4}^{\text{eff}}(\mathbf{k}, \mathbf{k}', \mathbf{q}, i\omega_m) \psi_{s_3}(\mathbf{k}', i\epsilon'_n) \psi_{s_4}(\mathbf{k}, i\epsilon_n), \quad (5)$$

where $\epsilon_n = (2n+1)\pi T$ is a fermionic Matsubara frequency, and the matrix element is

$$V_{s_1 s_2 s_3 s_4}^{\text{eff}}(\mathbf{k}, \mathbf{k}', \mathbf{q}, i\omega_m) = - \sum_{\mu, \nu=0,1} M_{\mu\nu}(\mathbf{k}, \mathbf{k}', \hat{\mathbf{q}}) [D_{+, \mu\nu}(q, i\omega_m) (\sigma_0)_{s_1 s_4} (\sigma_0)_{s_2 s_3} + D_{-, \mu\nu}(q, i\omega_m) (\sigma_3)_{s_1 s_4} (\sigma_3)_{s_2 s_3}], \quad (6)$$

with

$$M_{\mu\nu}(\mathbf{k}, \mathbf{k}', \hat{\mathbf{q}}) = \frac{1}{2} \begin{pmatrix} 1 & -i \frac{\hat{z} \cdot (\hat{\mathbf{q}} \times \mathbf{k}')}{m^*} \\ i \frac{\hat{z} \cdot (\hat{\mathbf{q}} \times \mathbf{k})}{m^*} & \frac{(\hat{\mathbf{q}} \times \mathbf{k}) \cdot (\hat{\mathbf{q}} \times \mathbf{k}')}{m^{*2}} \end{pmatrix}_{\mu\nu}, \quad (7)$$

which dictates the coupling of the Chern-Simons gauge field fluctuation to the CFs. Here the Pauli matrix σ_α ($\alpha = 0, \dots, 3$) acts on layer indices.

The dominant contribution in the effective interaction at small q comes from the out-of-phase fluctuation of the current-current correlation $D_{-,11}$. Preceding analysis explained the existence of a stable interlayer paired state by taking only the current-current propagator $D_{\pm,11}$ [17, 18]. However, this is not enough to examine the stable pairing symmetry because time-reversal symmetry breaking by the external magnetic field is absent. To this end, it is necessary to include the density-current propagators $D_{\pm,01}$ and $D_{\pm,10}$, which are induced by the Chern-Simons term and change sign under time reversal ($\tilde{\phi} \rightarrow -\tilde{\phi}$). In the following analysis, we include all terms in the effective interaction (6) on an equal footing.

Pairing symmetry and wave functions. We investigate the stable pairing state using the framework of the Eliashberg theory. Here the Green's function of the CFs in the Nambu space is written as

$$G^{-1}(\mathbf{k}, i\epsilon_n) = \begin{pmatrix} (i\epsilon_n Z_n - \xi_{\mathbf{k}}) \sigma_0 & \hat{\phi}_n(\mathbf{k}) \\ \hat{\phi}_n^\dagger(\mathbf{k}) & (i\epsilon_n Z_n - \xi_{\mathbf{k}}) \sigma_0 \end{pmatrix}, \quad (8)$$

where Z_n is the quasiparticle residue, $\hat{\phi}_n(\mathbf{k})$ is the anomalous self-energy, and $\xi_{\mathbf{k}} = \epsilon_{\mathbf{k}} - \mu$. The gap function is given by $\Delta_n(\mathbf{k}) = \hat{\phi}_n(\mathbf{k})/Z_n$. We focus on fully-gapped interlayer paired states. With the in-plane rotational symmetry, we have $\hat{\phi}_n^{(l)}(\mathbf{k}) = \phi_n(i\sigma_2)e^{i\theta_{\mathbf{k}}}$ (even l), or $\hat{\phi}_n^{(l)}(\mathbf{k}) = \phi_n(i\sigma_3\sigma_2)e^{i\theta_{\mathbf{k}}}$ (odd l), where l is the relative angular momentum and $\theta_{\mathbf{k}}$ is the azimuth of \mathbf{k} [25].

The Green's function $G(\mathbf{k}, i\epsilon_n)$ yields the effective action for the CFs. Recalling the BCS theory, we obtain the ground state of the CFs as

$$|\Psi_{\text{CF}}\rangle \propto \prod_{\mathbf{k}} (1 + g_{\mathbf{k}} c_{\mathbf{k}\uparrow}^\dagger c_{-\mathbf{k}\downarrow}^\dagger) |0\rangle. \quad (9)$$

$|0\rangle$ is the vacuum containing no particles, $c_{\mathbf{k}s}^\dagger$ creates a CF of momentum \mathbf{k} on layer s , and the function $g_{\mathbf{k}}$ is $g_{\mathbf{k}} = \phi_n e^{i\theta_{\mathbf{k}}} / (\xi_{\mathbf{k}} + E_{\mathbf{k}})$, with $E_{\mathbf{k}} = \sqrt{\xi_{\mathbf{k}}^2 + |\phi_n|^2}$ [24]. The wave function of a system with N electrons in each layer is obtained by

$$\Psi_{\text{CF}}(\{\mathbf{r}_\uparrow\}, \{\mathbf{r}_\downarrow\}) = \det[g(\mathbf{r}_{i\uparrow}, \mathbf{r}_{j\downarrow})], \quad (10)$$

where $g(\mathbf{r}_{i\uparrow}, \mathbf{r}_{j\downarrow})$ is the Fourier transform of $g_{\mathbf{k}}$; $g(\mathbf{r}_{i\uparrow}, \mathbf{r}_{j\downarrow}) = L^{-2} \sum_{\mathbf{k}} g_{\mathbf{k}} e^{i\mathbf{k} \cdot (\mathbf{r}_{i\uparrow} - \mathbf{r}_{j\downarrow})}$ (L^2 : the area of the system).

The electron wave function for an interlayer paired state generally has a form

$$\Psi(\{z\}, \{w\}) = \mathcal{P}_{\text{LLL}} \prod_{i < j} (z_i - z_j)^{\tilde{\phi}} \prod_{i' < j'} (w_{i'} - w_{j'})^{\tilde{\phi}} \times \det[g(z_i, w_j)], \quad (11)$$

where \mathcal{P}_{LLL} is the projection operator onto the lowest Landau level. Here we introduce the complex representations of the coordinate $z_i = x_{i\uparrow} - iy_{i\uparrow}$ and $w_j = x_{j\downarrow} - iy_{j\downarrow}$ [26]. The first two terms in the right-hand side describe the fluxes attached to the electrons. With an even $\tilde{\phi}$, this bosonic part corresponds to the Halperin $(\tilde{\phi}, \tilde{\phi}, 0)$ state [27]. For an interlayer paired state with an angular momentum l , we have $g(z_i, w_j) \sim (z_i - w_j)^{-l}$ in short distances [24], which produces a winding phase $2\pi l$; see Fig. 1(a). Using the Cauchy identity, the paired CF part can be regarded as the $(l, l, -l)$ state for a weak-pairing case [28].

Energetics of paired states. The quasiparticle residue Z_n receives a correction from the exchange interaction

$$V_{\text{ex}}(\mathbf{k}, \mathbf{q}, i\omega_m) = - \sum_{\mu\nu} M_{\mu\nu}(\mathbf{k}, \mathbf{k} + \mathbf{q}, \hat{\mathbf{q}}) [D_{+, \mu\nu}(q, i\omega_m) + D_{-, \mu\nu}(q, i\omega_m)], \quad (12)$$

and the anomalous self-energy $\hat{\phi}_n(\mathbf{k})$ is related to the interaction in the Cooper channel

$$V_c(\mathbf{k}, \mathbf{q}, i\omega_m) = \sum_{\mu\nu} M_{\mu\nu}(\mathbf{k}, -\mathbf{k} - \mathbf{q}, \hat{\mathbf{q}}) [D_{+, \mu\nu}(q, i\omega_m) - D_{-, \mu\nu}(q, i\omega_m)]. \quad (13)$$

In the Cooper channel, D_+ and D_- have the different signs, which reflects the fact that the two layers have the opposite $a^{(-)}$ gauge charges. Importantly, off-diagonal terms in $M_{\mu\nu}$, which correspond to density-current interactions and break time-reversal symmetry, affect only V_c .

We assume $\Delta_n(\mathbf{k}) \ll \epsilon_F$, so that the pairing occurs only on the Fermi surface. Then we define the effective coupling constants for Z_n and $\hat{\phi}_n^{(l)}(\mathbf{k})$ as $\lambda_{Z,m}$ and $\lambda_{\phi,m}^{(l)}$, respectively:

$$\lambda_{Z,m} = \int \frac{d^2q}{(2\pi)^2} \delta(\xi_{\mathbf{k}+\mathbf{q}}) V_{\text{ex}}(\mathbf{k}, \mathbf{q}, i\omega_m),$$

$$\lambda_{\phi,m}^{(l)} = \int \frac{d^2q}{(2\pi)^2} \delta(\xi_{\mathbf{k}+\mathbf{q}}) V_c(\mathbf{k}, \mathbf{q}, i\omega_m) \left(1 + \frac{q}{k_F} e^{i\theta_{\mathbf{q}}}\right)^l, \quad (14)$$

with the condition $|\mathbf{k}| = k_F$. The effective coupling constants are related to the Eliashberg equations [24]

$$(1 - Z_n) \epsilon_n = -\pi T \sum_{\omega_m} \frac{\lambda_{Z,m} Z_{n+m}(\epsilon_n + \omega_m)}{\sqrt{Z_{n+m}^2(\epsilon_n + \omega_m)^2 + |\phi_{n+m}^{(l)}|^2}},$$

$$\phi_n^{(l)} = -\pi T \sum_{\omega_m} \frac{\lambda_{\phi,m}^{(l)} \phi_{n+m}^{(l)}}{\sqrt{Z_{n+m}^2(\epsilon_n + \omega_m)^2 + |\phi_{n+m}^{(l)}|^2}}. \quad (15)$$

The stable pairing symmetry can be examined from $\lambda_{\phi,m}^{(l)}$, shown in Figs. 2(a)-(c). The integrations in Eq. (14) have divergences as $q \rightarrow 0$, and a cutoff $q_c = 10^{-5} k_F$ is introduced to cure them [24]. Negative values of $\lambda_{\phi,m}^{(l)}$ mean attractive interaction at ω_m , and the stable pairing symmetry will be the one that has the strongest attractive interaction.

The differences of the effective coupling constants $\Delta\lambda_{\phi,m}^{(l)} = \lambda_{\phi,m}^{(l)} - \lambda_{\phi,m}^{(0)}$ clearly display the stable pairing symmetry [Figs. 2(d)-(f)]. They do not have a singularity, and hence the cutoff is not necessary. We find that the $l = +1$ state is favored at all frequencies when the filling fraction is $\nu = \frac{1}{2} + \frac{1}{2}$ or $\frac{1}{4} + \frac{1}{4}$. The result suggests that a Cooper pair in the interlayer paired phase has an angular momentum $l = +1$. In contrast, the $l = 0$ state is favored at small frequencies for $\nu = \frac{1}{6} + \frac{1}{6}$. We note that the degeneracy of the states with $\pm l$ is lifted since the time-reversal symmetry is broken due to the coupling of the density and current fluctuations via the Chern-Simons term.

The layer spacing and the effective mass dependences of $\Delta\lambda_{\phi,m}^{(l)}$ at $\nu = \frac{1}{2} + \frac{1}{2}$ are also examined (Fig. 3). As the layer spacing d decreases, the differences of $\Delta\lambda_{\phi,m}^{(l)}$ increase, but the ordering remains unchanged. Controlling $(e^2/\epsilon l_0)/\epsilon_F$, proportional to the effective mass m^* , also does not change the ordering of $\Delta\lambda_{\phi,m}^{(l)}$. Similar results for other filling fractions are provided in Supplemental Material [24].

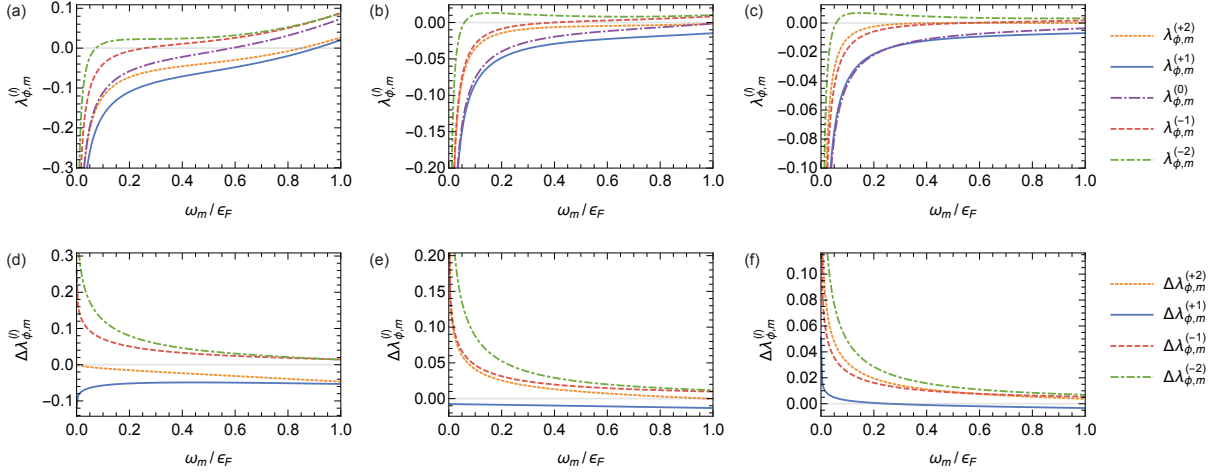


FIG. 2: Frequency dependence of (a)-(c) the effective coupling constants $\lambda_{\phi,m}^{(l)}$ and (d)-(f) the difference $\Delta\lambda_{\phi,m}^{(l)} = \lambda_{\phi,m}^{(l)} - \lambda_{\phi,m}^{(0)}$. We set the filling fraction (a), (d) $\nu = \frac{1}{2} + \frac{1}{2}$, (b), (e) $\nu = \frac{1}{4} + \frac{1}{4}$, and (c), (f) $\nu = \frac{1}{6} + \frac{1}{6}$. The ratio of the Coulomb energy to the Fermi energy is $(e^2/\epsilon l_0)/\epsilon_F = 1$ and the layer spacing is $k_F d = 1$. At filling $\nu = \frac{1}{2} + \frac{1}{2}$ and $\frac{1}{4} + \frac{1}{4}$, the $l = +1$ state is favored for all frequencies. In contrast, the $l = 0$ pairing is stable for low frequencies at $\nu = \frac{1}{6} + \frac{1}{6}$.

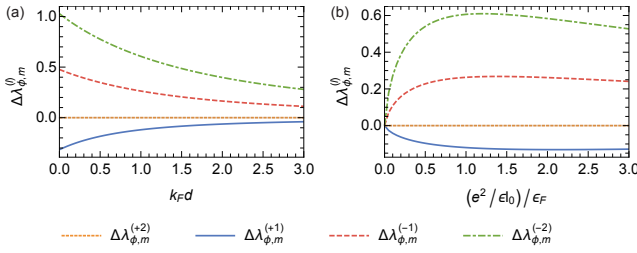


FIG. 3: (a) Layer spacing dependence of $\Delta\lambda_{\phi,m}^{(l)}$. We set $(e^2/\epsilon l_0)/\epsilon_F = 1$ and $\omega_m = 0$ at $\nu = \frac{1}{2} + \frac{1}{2}$. Reducing the spacing makes the interaction strength stronger. (b) Effective mass dependence of $\Delta\lambda_{\phi,m}^{(l)}$. Note $m^* \propto (e^2/\epsilon l_0)/\epsilon_F$. We set $k_F d = 1$ and $\omega_m = 0$ at $\nu = \frac{1}{2} + \frac{1}{2}$. In both cases, the ordering of $\Delta\lambda_{\phi,m}^{(l)}$ does not change. At $\nu = \frac{1}{2} + \frac{1}{2}$, the $l = +1$ pairing is favored at any cases. $\Delta\lambda_{\phi,0}^{(+2)}$ identically vanishes for $\tilde{\phi} = 2$. See also Eq. (17).

Discussions. It is instructive to examine $\lambda_{\phi,m}^{(l)}$ using the small- q expansion of $V_c(\mathbf{k}, \mathbf{q}, i\omega_m)$. A formation of a paired state is explained by considering the singular terms at $\omega_m = 0$:

$$\lambda_{\phi,0}^{(l)} = \frac{1}{(2\pi)^2} \frac{k_F}{m^*} \int_0^{2k_F} dq \left[-\frac{1}{\tilde{\chi}dq^2} + \frac{1}{\frac{e^2}{\pi\epsilon\tilde{\phi}^2}q} + O(q^0) \right], \quad (16)$$

which is independent of pairing symmetries. These singularities are smeared at finite frequencies, see Eq. (4). $\lambda_{Z,m}$ also has the similar structure, but it does not disturb a formation of pairing [29]. The first term represents attractive interaction originated from the out-of-phase fluctuation $a_1^{(-)}$ because $a_\mu^{(-)}$ sees the CFs in the differ-

ent layers as oppositely charged. The second term comes from the in-phase fluctuation $a_1^{(+)}$, which gives repulsive interaction.

In Eq. (16), the effect of the Chern-Simons term and hence time-reversal symmetry breaking is absent in the singular terms. The difference is found from q^0 order; we obtain

$$\Delta\lambda_{\phi,0}^{(l)} = \frac{1}{4\pi^2 k_F} \int dq \left[\frac{1}{2\tilde{\chi}dm^*} \left(l^2 - \frac{4l}{\tilde{\phi}} \right) + O(q) \right] \quad (17)$$

for $qd \ll 1$. It gives a good guideline for understanding the stable pairing symmetry. The quantity $l^2 - 4l/\tilde{\phi}$ is negative for $\tilde{\phi} = 2$ and $l = +1$, which explains negative $\Delta\lambda_{\phi,m}^{(l)}$ at $\nu = \frac{1}{2} + \frac{1}{2}$. It also nicely dictates the ordering of $\Delta\lambda_{\phi,m}^{(l)}$ at low frequencies, while higher order corrections should be considered if $l^2 - 4l/\tilde{\phi} = 0$. For example, at $\nu = \frac{1}{4} + \frac{1}{4}$, $l = +1$ gives $l^2 - 4l/\tilde{\phi} = 0$, but still the $l = +1$ state is favored.

The small- q expansion (17) moreover reveals the mechanism of stabilizing the $l = +1$ state. The l^2 term originates from the current-current interaction and the $4l/\tilde{\phi}$ term from the density-current interaction. Both are mediated by the out-of-phase gauge fluctuation. Since the current-current interaction is isotropic, it favors the $l = 0$ state and increases the energy of paired states with higher angular momentum. In contrast, the density-current interaction can be attractive or repulsive depending on the direction of the external magnetic field and the pairing symmetry. If it is attractive and exceeds the repulsion for the $l \neq 0$ states, there is a chance of pairing with finite orbital angular momentum. This occurs only for $l = +1$ and $\tilde{\phi} \leq 4$ (provided $\tilde{\phi} > 0$), which explains the stable $l = +1$ state.

The $l = +1$ state of CFs has the opposite angular momentum to the fluxes attached to electrons. This is seen from the electron wave function [Eq. (11)]. For small distances, it has a form

$$\Psi(\{z\}, \{w\}) \approx \prod_{i < j} (z_i - z_j)^{\tilde{\phi}} \prod_{i' < j'} (w_{i'} - w_{j'})^{\tilde{\phi}} \cdot \det \left(\frac{1}{z_i - w_j} \right), \quad (18)$$

which shows the opposite angular momenta for the fluxes and interlayer pairing.

Our finding of the interlayer paired state with $l = +1$ at large layer spacing is consistent with a preceding study [30], which estimated the pairing symmetry within the BCS theory. The properties of this $l = +1$ state are studied also in Ref. [22] without energetics. On the other hand, numerical studies of finite size quantum Hall bilayers on a sphere seem to infer a paired CF phase of $l = -1$ interlayer paired state at $\nu = \frac{1}{2} + \frac{1}{2}$ [31, 32]. This $l = -1$ state was found to be an exciton condensate by a very recent paper [33], which preserves the particle-hole symmetry of half-filled Landau levels. Here we focus on the time-reversal symmetry breaking due to the external magnetic field, instead of the particle-hole symmetry, only present in the case of $\nu = \frac{1}{2} + \frac{1}{2}$. The origin of the discrepancy in the stable pairing channel is presently unclear.

Conclusion. We have studied the pairing symmetry of interlayer paired states in quantum Hall bilayers by taking into account of the density and current fluctuations of CFs, and have found the $l = +1$ pairing is energetically favored at the filling fraction $\nu = \frac{1}{2} + \frac{1}{2}$ and $\frac{1}{4} + \frac{1}{4}$. The Chern-Simons term couples the density and current fluctuations, which breaks the time-reversal symmetry to lift the degeneracy of $\pm l$ states.

Acknowledgment. We thank A. V. Chubukov, T. Senthil, and I. Sodemann for valuable discussions. This work is supported by DOE Office of Basic Energy Sciences, Division of Materials Sciences and Engineering under Award DE-SC0010526.

-
- [1] J. K. Jain, Phys. Rev. Lett. **63**, 199 (1989); Phys. Rev. B **40**, 8079 (1989); Phys. Rev. B **41**, 7653 (1990).
[2] B. I. Halperin, P. A. Lee, and N. Read, Phys. Rev. B **47**, 7312 (1993).
[3] Y. W. Suen, L. W. Engel, M. B. Santos, M. Shayegan, and D. C. Tsui, Phys. Rev. Lett. **68**, 1379 (1992).
[4] J. P. Eisenstein, G. S. Boebinger, L. N. Pfeiffer, K. W. West, and S. He, Phys. Rev. Lett. **68**, 1383 (1992).
[5] D.-K. Ki, V. I. Fal'ko, D. A. Abanin, and A. F. Morpurgo, Nano Lett. **14**, 2135 (2014).
[6] A. Kou, B. E. Feldman, A. J. Levin, B. I. Halperin, K. Watanabe, T. Taniguchi, and A. Yacoby, Science **345**, 55 (2014).
[7] P. Maher, L. Wang, Y. Gao, C. Forsythe, T. Taniguchi, K. Watanabe, D. Abanin, Z. Papi, P. Cadden-Zimansky, J. Hone, P. Kim, and C. R. Dean, Science **345**, 61 (2014).
[8] Y. Kim, D. S. Lee, S. Jung, V. Skákalová, T. Taniguchi, K. Watanabe, J. S. Kim, and J. H. Smet, Nano Lett. **15**, 7445 (2015).
[9] I. B. Spielman, J. P. Eisenstein, L. N. Pfeiffer, and K. W. West, Phys. Rev. Lett. **87**, 036803 (2001).
[10] L. Tiemann, W. Dietsche, M. Hauser, and K. von Klitzing, New J. Phys. **10**, 45018 (2008).
[11] M. Kellogg, I. B. Spielman, J. P. Eisenstein, L. N. Pfeiffer, and K. W. West, Phys. Rev. Lett. **88**, 126804 (2002).
[12] M. Kellogg, J. P. Eisenstein, L. N. Pfeiffer, and K. W. West, Phys. Rev. Lett. **93**, 036801 (2004).
[13] E. Tutuc, M. Shayegan, and D. A. Huse, Phys. Rev. Lett. **93**, 036802 (2004).
[14] A. H. MacDonald, Physica B **298**, 129 (2001).
[15] J.-J. Su and A. H. MacDonald, Nat. Phys. **4**, 799 (2008).
[16] For a review of experiments of quantum Hall bilayers, see J. P. Eisenstein, Annu. Rev. Condens. Matter Phys. **5**, 159 (2014).
[17] N. E. Bonesteel, Phys. Rev. B **48**, 11484 (1993).
[18] N. E. Bonesteel, I. A. McDonald, and C. Nayak, Phys. Rev. Lett. **77**, 3009 (1996).
[19] G. Moore and N. Read, Nucl. Phys. **B360**, 362 (1991).
[20] In an experiment, gate electrodes adjacent to CF layers could screen the long-range Coulomb interaction and suppress the charge density fluctuation. Such a screening effect in bilayer graphene experiments is discussed in Ref. [21], for example.
[21] L. A. Ponomarenko, A. K. Geim, A. A. Zhukov, R. Jalil, S. V. Morozov, K. S. Novoselov, I. V. Grigorieva, E. H. Hill, V. V. Cheianov, V. I. Fal'ko, K. Watanabe, T. Taniguchi, and R. V. Gorbachev, Nat. Phys. **7**, 958 (2011).
[22] Y. B. Kim, C. Nayak, E. Demler, N. Read, and S. Das Sarma, Phys. Rev. B **63**, 205315 (2001).
[23] R. Cipri and N. E. Bonesteel, Phys. Rev. B **89**, 085109 (2014).
[24] See Supplemental Material, which includes Refs. [18, 22, 23, 28], for the derivations of the RPA gauge propagator and the Eliashberg equations, the detailed analysis of the effective coupling constants, and the discussion on the wave function of paired states.
[25] States with even l are spin-singlet pairings, while those with odd l are spin-triplet states, where “spin” corresponds to layer in the present model. The spin component of spin-singlet states is dictated by $i\sigma_2$, which corresponds to interlayer singlet pairing in bilayer systems. On the other hand, spin-triplet states still have spin degrees of freedom, but since we focus on interlayer pairings, their spin components are described by $\sigma_3(i\sigma_2)$, where a corresponding d -vector is $\mathbf{d} \propto e^{i\theta_{\mathbf{k}}} \hat{z}$.
[26] The definitions of the complex representation of the coordinate z_i and w_j depend on the sign of a product eB . The definitions here correspond to the case with $eB > 0$. In contrast, if we had $eB < 0$, the choice would be $z_i = x_{i\uparrow} + iy_{i\uparrow}$ and $w_j = x_{j\downarrow} + iy_{j\downarrow}$.
[27] B. I. Halperin, Helv. Phys. Acta **56**, 75 (1983).
[28] N. Read and D. Green, Phys. Rev. B **61**, 10267 (2000).
[29] Y. Wang, A. Abanov, B. L. Altshuler, E. A. Yuzbashyan, and A. V. Chubukov, Phys. Rev. Lett. **117**, 157001.
[30] T. Morinari, Phys. Rev. B **59**, 7320 (1999).
[31] G. Möller, S. H. Simon, and E. H. Rezayi, Phys. Rev. Lett. **101**, 176803 (2008).
[32] G. Möller, S. H. Simon, and E. H. Rezayi, Phys. Rev. B

79, 125106 (2009).

[33] I. Sodemann, I. Kimchi, C. Wang, and T. Senthil,

arXiv:1609.08616.